# Interference Identification and Resource Management in OFDMA Femtocell Networks

Chin-Jung Liu, Pei Huang, Li Xiao, Abdol-Hossein Esfahanian
Department of Computer Science and Engineering,
Michigan State University, East Lansing, MI 48823, USA
{liuchinj, huangpe3, lxiao, esfahanian}@cse.msu.edu

***Abstract*—Inter-femtocell interference significantly limits the achievable throughput of an OFDMA femtocell system, which calls for interference management tailored for femtocell networks. A typical approach to mitigate inter-femtocell interference is known as resource isolation, which aims at assigning non-overlapping resources to interfering femtocells. One of the main challenges for interference mitigation in femtocell networks is that the femtocells are often installed by end-consumers without any pre-planning. Very limited information about the femtocells is available, making it hard to decipher the inter-femtocell interference. In this paper, we propose an efficient method to identify inter-femtocell interference by analyzing the received patterns observed by mobile stations. We conducted experiments to demonstrate that the proposed interference identification method can successfully identify real interferers while excluding non-interfering femtocells from suspicious interferers. Based on the proposed interference identification, we propose a weighted vertex-coloring based resource assignment algorithm to allocate resources with better fairness and achieve higher throughput.**

## I. Introduction

Although cellular networks provide almost ubiquitous coverage in most areas, complaints of low-quality service in terms of signal reception are often reported by indoor users. Signal attenuations are mainly attributed to the penetration losses through building structures and multipath propagation. To improve the indoor service quality and coverage, low-power and low-cost indoor cellular base stations called femtocells [1] have been deployed. Femtocells operate in the same licensed spectrum band and use the same technology as macrocell infrastructures, hence no modification to existing devices are required. Several Orthogonal Frequency Division Multiple Access (OFDMA [2]) based 4G cellular network standards such as WiMAX and LTE-A have endorsed femtocell as a mandatory technology. Femtocells attach to the core cellular network via IP-based broadband backhauls. Femtocells are promising in terms of providing superior voice quality and higher data rates for indoor users. Large-scale deployment of femtocells in urban area is expected to be realized in the future.

Due to the fact that all base stations operate in the same licensed spectrum band, inter-cell interference (including inter-femtocell and cross-tier macrocell/femtocell interference) significantly limits the achievable throughput of a femtocell cellular network. A typical approach to mitigate inter-cell interference is known as resource isolation, which assigns non-overlapping resources to interfering stations. To mitigate interference, the most critical step is to identify the interference relations in the network.

ISBN 978-3-901882-58-6 

Macrocells are installed by service providers with careful planning, thus inter-macrocell interference is minimized at coverage edges. Interference management between macrocells and femtocells is also widely studied [3][4][5] where the locations of macrocell base stations are known. In this paper, we focus on a more challenging problem, which is the inter-femtocell resource management. Several characteristics of femtocells make the interference identification challenging. The femtocells are often installed by end-consumers without any pre-planning. An individual femtocell possesses no information as to either its own location or the existence of nearby femtocells. Since very limited information about the femtocells is available, it is hard to decipher the inter-femtocell interference. In addition, it is unrealistic to expect the coordination and assistance from the user devices because the goal of femtocell cellular network is to augment the coverage without modifying any existing user devices.

Several efforts have been made to improve inter-femtocell resource management. Authors in [6] propose to let femtocells assign resources to mobile stations (MSs, e.g., cellphones and tablets) based on a hashing method. If an MS is experiencing interference in certain resources, the femtocell invokes a collision resolution procedure and tries to assign the MS other resources. The collision resolution procedure does not require the identification of interferer, but it may require a certain amount of subsequent frames to find available resources. FERMI [7] introduces two dedicated measurement zones in a frame. If an MS is experiencing interference, the delivery rates of the two zones would be significantly different. A central controller determines whether an MS experiences interference by observing the difference between the delivery rates in the two zones. If the MS were experiencing interference, the femtocell considers all nearby femtocells whose *received signal strength (RSS)* is over a threshold as interferers. This approach is highly sensitive to the threshold of the RSS [8] and it is extremely difficult to determine a uniform threshold across the whole network.

Instead of using the RSS, we propose to improve the interference identification by taking advantage of the availability of multiple subchannels in an OFDMA system. We let each femtocell transmit data using a subset of subchannels. The different combinations of subchannels are called *patterns* in

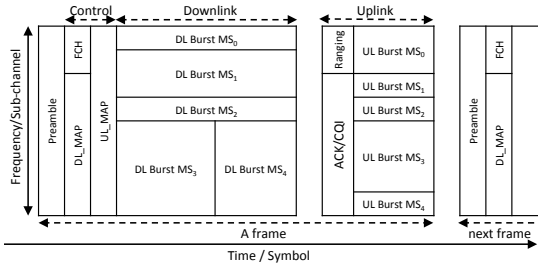


Fig. 1: WiMAX frame structure.

our paper. Femtocells transmit with different transmission patterns, which impact the subchannels the MSs can receive data from. The subchannels from which an MS receives data constitute a received pattern. The proposed interference identification algorithm identifies the interference relations in the network by examining these patterns intelligently. Experiments on GNURadio/USRP are conducted to demonstrate the unique received patterns observed by the MSs. The results show that our method successfully identifies all real interferers and most non-interfering femtocells.

Because the method identifies real interferers while excluding non-interfering femtocells, the number of edges in the conflict graph is reduced and the achievable throughput is improved. Further, we propose an efficient weighted vertex-coloring based resource assignment algorithm that allocates resources with better fairness and achieves higher throughput.

The rest of this paper is organized as follows. Section II provides a brief introduction on the background of OFDMA systems and discussions on related work. We give an overview of our interference identification algorithm and describe the experiment to prove our concept in Section III. Details about interference identification are presented in Section IV. In Section V, we explain our algorithm for resource management. Section VI is devoted to evaluate our interference identification and the resource management algorithm. Finally, we draw a conclusion in Section VII.

## II. Background Overview and Related Work

In this section, we briefly introduce the background of OFDMA systems and some related work.

### A. Background Overview

In an OFDMA system, the radio resources are two-dimensional frames of frequency (subchannel) and time (symbol). An OFDMA device operates in all or partial of orthogonal subchannels in each frame. Continuous spectrum is divided into multiple equally spaced tones (subcarriers) and several subcarriers are grouped to form a subchannel. Several time symbols in a subchannel form a *resource block (RB)*.

Figure 1 shows a WiMAX Time Division Duplex (TDD) frame, where horizontal axis denotes the time and vertical axis denotes the frequency. A TDD frame has a fixed duration and is composed of a downlink (DL) and an uplink (UL) sub-frame. DL also contains a control part, which includes preamble, FCH (Frame Control Header) and downlink map (DL_MAP). When the base station transmits a frame, all MSs that are associated with this base station receive this frame. The DL_MAP in the control part informs MSs of the RB assignments and their modulation and coding scheme (MCS) in the downlink. The DL_MAP is protected by the most robust MCS. An MS knows which RB belongs to it from the DL_MAP. MSs acknowledge (ACKs) the reception of each RB through the dedicated subchannels in UL.

### B. OFDMA Systems Related Work

Macrocells are usually deployed by wireless service providers with careful planning, including location, height, frequency, and even antenna configuration. Therefore, inter-macrocell interference is minimized at coverage edges. Multi-cell OFDMA frequency planning is also discussed in [9][10], but these approaches require certain amount of knowledge of the base stations. Due to the fact that femtocells possess little knowledge of their information, frequency planning is not feasible for femtocell networks.

Interference management between macrocells and femtocells has been widely studied as well. In earlier generation cellular networks (e.g., CDMA and GSM), there is only one carrier. Interference management mainly rely on pure frequency isolation [5] or power auto-configuration [3][4]. Authors in [5] propose to arbitrarily assign different frequency spectrum to macrocells and femtocells. For OFDMA-based cellular networks, a centralized approach for managing interference between macrocells and femtocells is proposed in [6], which prevents femtocells from reusing the resources that are occupied by macrocells. In these work, the knowledge of macrocells is relatively easier to obtain. A distributed interference control for OFDMA-based cellular network through learning technique and power control is proposed in [11]. The agents learn an optimal power allocation policy by directly interacting with the surrounding environments.

A distributed hashing based inter-femtocell resource management is proposed in [6]. Femtocells assign resources to MSs by a random hashing scheme without any coordination with other femtocells. Collisions might occur if two interfering femtocells assign the same RB to their MSs. Due to the collision, the MS is unable to receive the RB correctly and the femtocell notices the interference through the ACK. A collision resolution procedure is thus proposed to resolve the collision, rehashing another available RB to the MS. The hashing scheme and the collision resolution procedure avoid the need of identifying the interference relations. However, the potential collision degrades the quality of service and it may take multiple subsequent frames to resolve one collided RB. In addition, it is possible that some RBs are mistakenly considered as collisions and trigger the rehashing unnecessarily.

In RADION [12], instead of assigning resources randomly, a probing method is proposed for the femtocells to search for available subchannels opportunistically. Each femtocell periodically transmits data bursts on certain resources and observes the difference of the *Burst Delivery Rate (BDR)* [7][12], which is defined as the number of bursts received at the client divide by the total number of bursts transmitted.

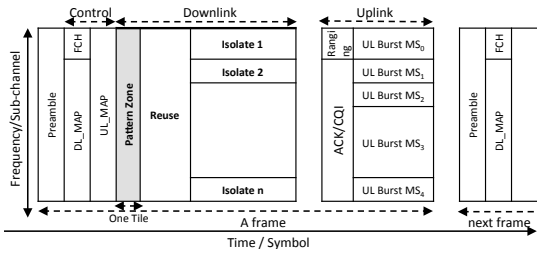


Fig. 2: Zoning in our design.

The resources with higher BDR are considered available and the femtocell assigns these resources to its client. However, the resource allocated to each client may result in fragmented spectrum and unfair resources allocation.

FERMI [7] introduces two dedicated measurement zones (*free* and *occupied* zones) in the downlink of a frame. In **free** zone, only $\gamma$ out of $n$ femtocells transmit using all subchannels. In **occupied** zone, *all* femtocells transmit using all subchannels. If an MS were experiencing interference, the BDR in the *occupied* zone will be significantly lower than the BDR in the *free* zone. Through comparisons between the BDR in free and occupied zone, the central controller infers the interference in the femtocell networks without knowing femtocells' information. An MS maintains a list of nearby cells for potential handovers and measures the RSS from these cells. If the central controller finds that an MS is experiencing interference, the corresponding femtocell considers all nearby femtocells with RSS over a threshold as interferers. However, relying on RSSs makes such interference identification highly sensitive to the threshold. It is also difficult to determine the threshold [8]. Especially for femtocell networks, the MSs are indoor and there are many factors that affect wireless links. Meanwhile, the indoor environment makes it impractical to use a universal threshold across the whole network.

## III. Interference Overview and Experiment

The goal of resource management is to assign downlink RBs to MSs with minimized interference, maximized throughput, and maximized fairness. To mitigate interference, the most critical step is to identify the interference relations in the network. Interference identification directly affects the performance of resource management. We propose an efficient method that takes advantage of the availability of multiple subchannels. As shown in Figure 2, we introduce a *pattern zone* in the DL part. The pattern zone is used to distinguish real interferers from non-interfering femtocells so that the throughput can be improved with fewer number of edges in the constructed conflict graph. Other OFDMA-based systems such as LTE-A also has similar frame structure and we can introduce similar pattern zone structure.

In the pattern zone, each femtocell transmits data using a subset of *n* subchannels. The interfering femtocells to an MS *m* will impact the received patterns on the MSs. Each femtocell extracts the received pattern on its MS from their ACKs. The received patterns of the MSs and the transmission patterns of the femtocells are collected at the central controller through the backhaul. The central controller identifies the interference relations in the network and builds a conflict graph. Resources are allocated based on the conflict graph.

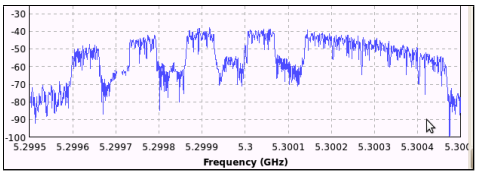


Fig. 3: The received RSS of a transmission pattern 01010101011111.

### A. Interference Experiment Setup

We conducted experiments to demonstrate that different transmission patterns from interferers do affect the received patterns on the MSs. Although commercial OFDMA-based cellular services have been already deployed in many countries, we have no access to commercial femtocells and their proprietary software. Therefore, we implemented a subset of OFDMA system on GNU Radio [13] and USRP [14] to prove our concept. Since we cannot access the licensed spectrum band, our experiment is conducted at 5.3 GHz. The system bandwidth is 1 MHz and the modulation is BPSK. We split the frequency into 256 tones and thus each subcarrier has a bandwidth of 3.90625 kHz. We do not use the central 2 subcarriers due to the DC-offset and we skip 8 subcarriers at two ends because of the roll down of filters.

For downlinks, we group 16 subcarriers into one subchannel and this partition forms 14 subchannels in total. We also spare one subcarrier between two subchannels as a small guard band to avoid cross-subchannel interference. We define one RB as a subchannel over 6 symbols and an RB carries 96 bits. (BPSK carries 1 bit per symbol.) In order to examine if an RB is received correctly, we reserve 4 bytes for CRC and 8 bytes are left for data. When receiving an RB, the receiver determines whether the RB is received correctly by checking whether the received data matches CRC.

As shown in Figure 2, the pattern zone is defined as one RB over all subchannels in each frame. Each femtocell $f$ generates a random pattern in pattern zone by only utilizing a subset of $n$ subchannels. Let us denote the transmission pattern from femtocell $f$ as a string $p_{tx}(f) = c_1c_2...c_n$, where $c_i = 1$ if subchannel $i$ is occupied by $f$, otherwise $c_i = 0$. A *bit* in the pattern $c_i$ is denoted as $p_{tx}(f)[i]$ and the length of a pattern $p$ is denoted as $|p|$. If $p_{tx}(f)[i] = 1$, the subchannel $i$ is used for transmission, otherwise, the subchannel $i$ is left idle. In our implementation, there are 14 subchannels. Figure 3 illustrates the RSS of a transmission pattern $p_{tx} = 01010101011111$. Let us also denote the received pattern on an MS $m$ as a string $p_{rx}(m) = c_1c_2...c_n$, where $c_i$ is marked as 1 if the RB in subchannel $i$ is received correctly, otherwise $c_i$ is marked as 0. If the RB carried by subchannel $i$ is not destined for this $m$, $c_i$ is also marked as 0. If a pattern is all 0 or all 1, we denote them as $0_n$ or $1_n$.

Our testbed is composed of three USRPs, one USRP1 as transmitting femtocell, $Tx$, one USRP E110 as receiving MS,

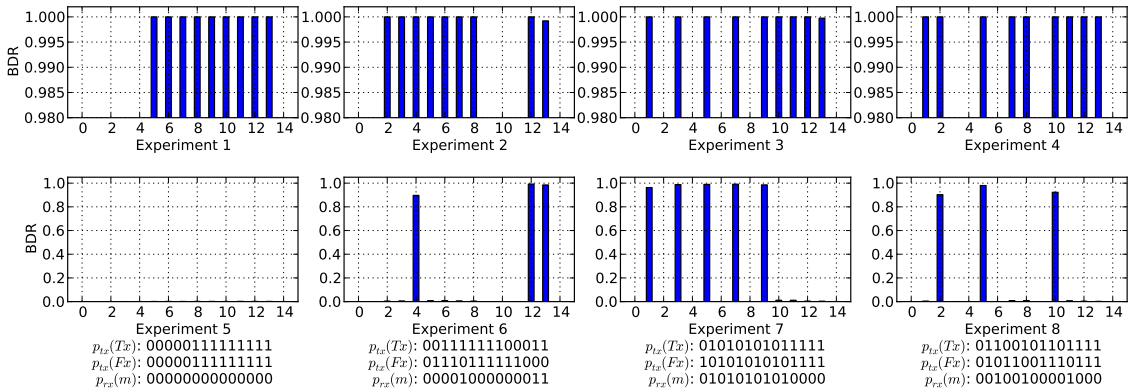


Fig. 4: The burst delivery rate (BDR) on each subchannel for four different transmission patterns.

$m$, and one USRP1 as interferer femtocell, $Fx$. $Tx$ and $m$ are 1.5 meters away and their antennae are 1 meter above the floor. The distance between $Tx$ and $Fx$ is 3 meters. The transmission gain of $Tx$ is set to 10 dBi and the receiver gain of $m$ is set to 10 dBi.

### *B. Interference Experiment*

We first conducted a set of experiments with no interferer and the transmitter $Tx$ transmits four representative transmission patterns. The received patterns on $m$ are shown in experiments 1 to 4 in Figure 4. Taking experiment 2 as an example, $p_{tx}(Tx) = 00111111100011$ indicates that $Tx$ does not transmit on subchannel 0, 1, 9, 10, and 11. These experiments demonstrate that when $m$ is interference-free, almost $100\%$ of the RBs are received correctly. If there is no interference at all, $p_{rx}(m)$ should be identical to $p_{tx}(Tx)$.

We then conducted another set of experiments that includes an interferer $Fx$, which also transmits four patterns. $Tx$ still transmits using the original four patterns. $Tx$, $m$ and $Fx$ are placed in a straight line in the same order. The transmission gain of $Fx$ is set to 5 dBi. The results from experiments 5 to 8 are shown in Figure 4. In experiment 5, the $p_{tx}(Tx)$ is exactly the same as $p_{tx}(Fx)$ and thus $p_{rx}(m)$ is expected to be $0_n$, which is confirmed by the result. Collisions happen in all subchannels and those BDRs are $\approx 0\%$. From experiments 5 to 8, we observe that for subchannels occupied by both $Tx$ and $Fx$, the BDRs are $\approx 0\%$. For subchannel that is occupied by $Tx$ but not by $Fx$, $m$ still receives most of the RBs correctly. However, the BDR of subchannel 4 in experiment 6 and subchannel 2 in experiment 8 drops to around 90% because several adjacent subchannels are subject to interference.

The experiment result shows that the receive patterns on the MS do reflect the existence of interferers. By examining these $p_{rx}$s and $p_{tx}$s as introduced below, we can decipher the interference relations in a femtocell network.

## IV. Interference Identification Algorithm

The experiments above show that the interference can be identified from the subchannel BDR difference. This section introduces the interference identification algorithm that finds out which interferer causes the interference. Consider a femtocell network that consists of a set of femtocells $F$ and a set of MSs $M$. The femtocell to which an MS $m$ is associated is denoted by $f(m)$. $m$ can only receive RB from $f(m)$ and $f(m)$ is the only $Tx$ to $m$. All other transmissions from $f \in (F - f(m))$ are considered potential interference signals.

In the pattern zone of each frame, every femtocell $f$ transmits a randomly generated $p_{tx}(f)$. $m$ replies the ACKs about the reception of the RBs back to $f(m)$. According to these ACKs, $f(m)$ can extract the received pattern $p_{rx}(m)$. Each pattern can be represented as several integers depending on the length of the pattern. The system bandwidth in WiMAX can be 5, 10 or 20 MHz, which gives us $|p| = 15,\ 30$ or $60$. A pattern in WiMAX can be represented by one or two four-byte integers. All the transmission patterns $p_{tx}$s and received patterns $p_{rx}$s are gathered at a central controller through the backhaul. The central controller is responsible for identifying the inter-femtocell interference based on these patterns.

A requirement for the transmission patterns is that the number of 1s must be greater than the number of 0s ($\sum_{i=0}^{n-1} p_{tx}(f)[i] > \frac{n}{2}$). If the number of 1s is less than 0s, it is possible that two femtocells are interfering but their $p_{tx}$s do not have any overlapping subchannels. For example, the pattern $11111000000000$ and $00000000011111$ do not generate a pattern that is useful in interference identification. In contrast, if the number of 1s is greater than $\frac{n}{2}$, it is guaranteed that we have some colliding subchannels. Let the number of 1s be $k > \frac{n}{2}$ in any $p_{tx}$, the subchannel overlapping is guaranteed as $k + k > \frac{n}{2} + \frac{n}{2} = n$. It is guaranteed to have $2k - n$ overlapping subchannels. The relations between $p_{tx}(f(m))$ and $p_{rx}(m)$ reflect interference condition.

*1) $p_{tx}(f(m)) = p_{rx}(m)$:* The received pattern on $m$ is exactly the same as the transmission pattern from $f(m)$. The data carried by all subchannels are received correctly. Obviously, this $m$ is not experiencing any interference from nearby femtocells. It is classified as a class 1 MS. No further interference processing is needed.

*2) $p_{tx}(f(m)) \neq p_{rx}(m)$:* The femtocell $f(m)$ observes that $m$ receives a different pattern. For a subchannel $i$ occupied by $f(m)$ (i.e., $p_{tx}(f(m))[i] = 1$), it expects that $m$ receives the RB correctly and $p_{rx}[i]$ equals 1. If $p_{rx}[i]$ is not 1, it means that *there is an interferer whose $p_{tx}(Fx)[i]$ is 1*. The $m$ is classified as a class 2 MS. The interferers are identified through a process of elimination.

If $p_{rx}(m)[i] = 1$ and a suspicious interfering femtocell has $p_{tx}(f)[i] = 1$, the suspicious interfering femtocell $f$ is *not* a real interferer to $m$ or it is a weak interferer to $m$ because the transmission of the suspicious interferer does not cause a loss on the subchannel $i$. In cellular networks, the MSs maintain a list of nearby cells for potential handovers. Therefore, we only examine femtocells whose RSS at MS $m$ is above a certain *suspect threshold* $\theta$. We do not rely on this suspect threshold $\theta$ solely. Instead, we just list those femtocells as suspicious interferers. We denote the suspicious interferers as *suspect($m$)*. We exclude *non-interfering femtocells* from suspicious interferers based on *interference-free pattern* defined below.

**Definition 1** *The interference-free pattern between an MS m and a femtocell $f \neq f(m)$ is defined as $p_{free}(f, m) = p_{tx}(f) \cap p_{rx}(m)$. If $p_{free}(f, m) \neq 0_n$, $m$ is said to be interference-free from $f$ because even with the concurrent transmission of $f$, node $m$ is able to receive data correctly from its associated femtocell $f(m)$.*

The process of exclusion based on Definition 1 faces two problems. First, if a suspicious interferer femtocell $f$ generates a pattern that is exactly the same as $f(m)$, $p_{rx}(m)$ becomes $0_n$ because the interferer collides with $f(m)$ in all subchannels. If $p_{rx}(m) = 0_n$, for all other $f \in$*suspect($m$)*, $p_{free}(f, m) = 0_n$. All suspicious interferers are mistakenly considered as real interferers. Therefore, we require that the femtocells must generate disjoint random transmission patterns. This can be coordinated by the central controller.

Second, it is possible that a weak interferer does not introduce a clear interference pattern. Suppose $p_{tx}(Fx)$ is weak in experiment 8. The received pattern on $m$, $p_{rx}(m)$, may be 0010010$\underline{0}$10100$\underline{1}$ instead of 00100100001000. The interferer $Fx$ fails to cause significant $RB$ losses on two subchannels. The interference-free pattern $p_{free}(Fx, m) = 00000000100001 \neq 0_n$, which mistakenly identifies $m$ as interference-free from $Fx$. Therefore, depending on interference-free pattern solely is insufficient. To improve the accuracy, we add more strict constraints that can better identify interferers. We first define an interference pattern to identify subchannels that are experiencing interference.

**Definition 2** *The interference pattern on a mobile station m is defined as $p_{ix}(m) = \overline{p_{rx}(m)} \cap p_{tx}(f(m))$.*

$p_{ix}(m)[i] = 1$ indicates that the RB carried by subchannel $i$ is lost. In the case that $p_{rx}(m) = p_{tx}(f(m))$, all data are received correctly on all subchannels. The interference pattern $p_{ix}(m)$ should be $0_n$, which means that $m$ is interference-free to all femtocells and $m$ is a class 1 MS and *suspect($m$)* is empty. This is the condition 1 $p_{tx}(f(m)) = p_{rx}(m)$.

However, if $p_{ix}(m) \neq 0_n$, some subchannels are subject to interference. The $m$ is a class 2 MS. The next step is to figure out which suspicious interferer contributes to the interference.

**Definition 3** *The unique pattern of a suspicious interferer f is defined as $p_{ux}(f) = c_1 c_2 ... c_n$, where $c_i = 1$ if $p_{tx}(f)[i] = 1$ and for all $g \in \{suspect(m) - f\}$, $p_{tx}(g)[i] = 0$; otherwise, $c_i = 0$.*

The unique pattern $p_{ux}(f)$ denotes the subchannels that are *only* occupied by $f$. If $c_i$ in $p_{ux}(f)$ is 1, it means that $f$ is the only possible interferer that affects subchannel $i$. We define a conflict pattern $p_{cx}$ by comparing the unique patterns with the interference pattern.

**Definition 4** *$p_{cx}(f, m) = p_{ux}(f) \cap p_{ix}(m)$ is the conflict pattern on $m$ caused by $f$, where $c_i = 1$ means the RB loss in subchannel $i$ is definitely caused by $f$.*

From $p_{cx}$ we can infer which interferer is responsible for the RB loss in a certain subchannel. If $p_{cx}(f, m) \neq 0_n$, $f$ is a real interferer to $m$. We can also exclude non-interfering femtocells from suspicious interferers according to Definition 5.

**Definition 5** *$p_{irr}(f, m) = p_{ux}(f) \cap p_{rx}(m)$ is the irrelevant pattern of m caused by f, where $c_i = 1$ means $f$ is the only possible interferer, but m is not experiencing interference from $f$ as m still receives the RB correctly.*

Obviously, if $p_{irr}(Fx, m) \neq 0_n$, it means although some subchannels are occupied by both the $Fx$ and the $f(m)$, no collision is observed on $m$, confirming that $Fx$ is an non-interfering femtocell to $m$. In summary, we determine whether or not $m$ is experiencing interference from $f$ based on three criteria in the following order.

- $p_{cx}(f, m) \neq 0_n$, $f$ is a real interferer to $m$.
- $p_{irr}(f, m) \neq 0_n$, $f$ is a non-interfering femtocell to $m$.
- $p_{free}(f, m) \neq 0_n$: $m$ is interference-free from $f$.

In other words, in addition to the loose constraint in Definition 1, we first check whether there exist subchannels in which $f$ is the only suspicious interferer and RB loss is observed. If the condition is true, $f$ is definitely a real interferer to $m$; otherwise, we check whether $f$ can be excluded from suspicious interferers according to Definition 5. Finally, we use the interference-free pattern in Definition 1 to check whether $m$ is interference-free from $f$ if there is no such a subchannel where $f$ is the only suspicious interferer.

If all of the three criteria do not hold, the $f$ is conservatively considered as a real interferer. As mentioned earlier, we only examine *suspect($m$)* whose RSS at $m$ is above a threshold $\theta$. The worst case performance is bounded by identifying all $f \in$ *suspect($m$)* as real interferers to $m$. However, the decision is made based on several consecutive frames. The side effect of weak interferers and weak receivers is alleviated.

As mentioned in Section IV, each pattern is gathered in the central controllers through the backhaul and stored as several integers. The operations to the patterns in our algorithm are bitwise operations that take constant time. Therefore, the time consumption of processing the patterns in the central controller is $O(|M|)$, where $|M|$ is the number of MSs in the network.

**Building the conflict graph.** The central controller performs the interferer identification for each frame. The input to the interference identification algorithm is a network $N$

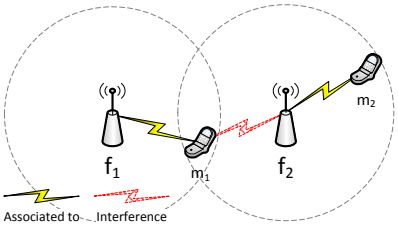


Fig. 5: Interference scenario.

and the output is a conflict graph $G$. Considering a femtocell network $N = \{F, M\}$ where $F$ is a set of femtocells and $M$ is a set of MSs, $|F|$ and $|M|$ denote the number of femtocells and MSs respectively. Each MS $m$ is associated with exactly one femtocell, denoted as $f(m)$. $m$ can only receive data from $f(m)$. Each $m$ puts the femtocells whose RSS at $m$ are greater than $\theta$ in the list of suspicious interferers, denoted by *suspect(m)*. For each $f$ in *suspect(m)*, we keep a history record $record_m(f)$, 1 denotes $f$ is a real interferer to $m$, 0 otherwise. If more than half of the records are 1, $f$ is regarded as a real interferer to $m$. The femtocells are modeled as vertices in $G = \{V, E\}$, where $V = F$. For $f$, $g \in F$, if $f$ is interfering with $g$, an edge $(f, g)$ is added to $E$. The weight of the vertex $w(f)$ is the number of class 2 MSs associated to $f$.

In each frame, every femtocell $f$ transmits a randomly generated unique $p_{tx}(f)$. From the ACKs of each $m$, $f(m)$ extracts the received pattern $p_{rx}(m)$. These $p_{tx}$s and $p_{rx}$s are forwarded to the central controller. The central controller infers the interference relationships by applying the three rules and build the conflict graph. Based on the conflict graph, the central controller assigns isolated resource to interferer femtocells, which will be discussed in Section V.

## V. Resource Allocation and Assignment

Because there are class 1 MSs that do not experience interference from any femtocell, their associated femtocell base stations can transmit data to them at the same time. The transmission period is thus divided into *reuse zone* and *isolation zone* similar to FERMI [7] as shown in Figure 2. In the *reuse zone*, all interference-free femtocells transmit at the same time and the *isolation zone* is used by femtocells that are subject to interference. Compared with prior schemes that isolate resources for each femtocell, the structure is more efficient as interference-free femtocells are allowed to utilize the whole band. To maximize the benefit of *reuse zone*, accurate interference identification is critical.

The example in Figure 5 demonstrates the importance of interference identification. Assuming that $m_1$ is not experiencing interference from $f_2$, both $m_1$ and $m_2$ are class 1 MSs. $f_1$ can assign all resources to $m_1$ and $f_2$ can assign all resources to $m_2$. There is no need to isolate resources for them. They can reuse the same resource without interfering with each other.

However, if $f_2$ is *mistakenly* identified as a real interferer of $m_1$, $m_1$ and $m_2$ have to give up the *reuse zone* and compete with others in the *isolation zone*. The unnecessary resource isolation results in resource underutilization. Our interference identification algorithm introduced above aims at identifying real interferers and excluding non-interfering femtocells.

Based on the interference identification, interference-free femtocells can utilize the whole band at the same time in the *reuse zone*. For the *isolation zone*, we propose a weighted vertex-coloring (WVC) algorithm to allocate resources based on the conflict graph. The goal is to assign isolated resource blocks to the class 2 MSs in each femtocell with minimized interference and maximized resource utilization while maintaining weighted max-min fairness [15].

FERMI [7] proposes a resource assignment algorithm that assigns resource by identifying maximal cliques in the conflict graph and assigning the resources to the vertices in those maximal cliques. For general graphs, listing all maximal cliques takes exponential time, but for *chordal graphs*, listing all maximal cliques can be done in linear time. Therefore, they adopt an $O(|V| \cdot |E|)$ complexity triangulation algorithm [16] that converts general graphs into chordal graphs by adding *fill-in* edges. As long as the graph is chordal, FERMI guarantees to produce optimal assignment. However, adding an extra edge between two vertices $u$ and $v$ means $u$ and $v$ are also interfering with each other and they need resource isolation. The system needs to assign isolated resource to $u$ and $v$ even though they do not interfere with each other and thus the resource utilization is decreased. As the density of femtocell increases, the number of vertices increases and the number of *fill-in* edge increases drastically. In addition, the triangulation algorithm [16] involves paths with special property and is very time consuming in large graphs.

Since the conflict graphs are weighted graphs, we cannot merely formulate the problem as multi-coloring problem. We formulate the problem as a weighted vertex coloring problem (WVCP). Unlike graph coloring for Wi-Fi [17], we cannot model one subchannel as one color and minimize the number of color used. This is because a subchannel may be assigned to different mobile stations in different resource blocks in a frame. Moreover, if we model one subchannel as one color, the subchannel assignment to the vertices is bundled with the color class and results in *discontinuous* subchannel assignment. In our work, we model a color class as a set of nonadjacent vertices that can share the same *set of subchannels* without causing interference. Our WVC assignment algorithm is a two-pass procedure: (1) assign colors to all vertices in $G$ and (2) allocate and assign subchannel subsets to the vertices based on the color assigned.

A proper coloring $C$ of a weighted graph $G = (V, E)$ is $\{V_1, V_2, ...V_k\}$, where $V_i$ is a disjoint independent subset of $V$ and $V_1 \cup V_2 \cup ... \cup V_k = V$. An independent set $V_i$ in $G$ is a set of pairwise nonadjacent vertices. The weight of a vertex $V_i$ is denoted as $\alpha(V_i)$ and is defined as the maximum weight vertex in that $V_i$. The weight of $C$ is denoted as $W(C) = \sum_{i=0}^{k} \alpha(V_i)$. The goal is to minimize $W(C)$.

It is known that vertex coloring is NP-hard. We can reduce WVCP to vertex coloring by letting the weights on all vertices to 1. Therefore, we propose a heuristic algorithm that colors the vertices in the order of a breadth-first-search tree rooted

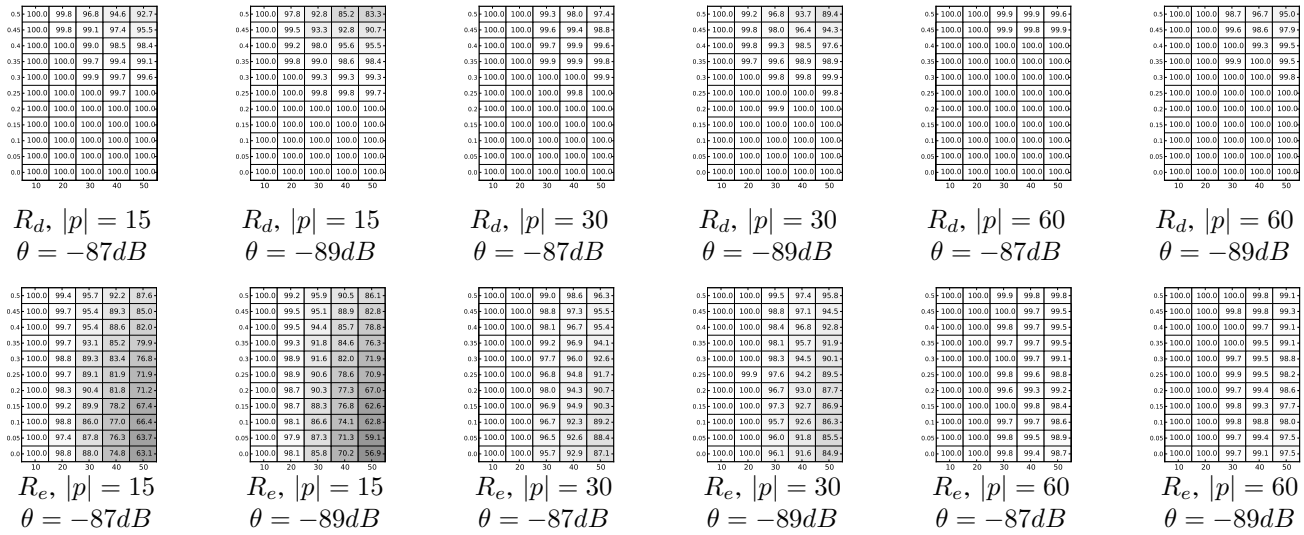


Fig. 6: The *detection rate* $R_d$ and *exclusion rate* $R_e$. $\theta$ is the *suspect threshold* and $|p|$ is the *pattern length*. X-axis denotes femtocell density settings in a ($500 \cdot 500$ $m^2$ area) and y-axis denotes *error probability* $P$.

at the highest degree vertex. When assigning a vertex $v$, we assign $v$ to the independent set $V_i$ such that the *increment of W(C) is minimized*. We check if $V_i$ can accommodate $v$ in the order of descending $\alpha(V_i)$. If none of these independent set can accommodate $v$, a new independent set $\{v\}$ is add to $C$.

After computing the independent sets $\{V_1, V_2, ...V_k\}$, we assign actual subchannel in the descending order of $w(v)$ in each independent set $V_i$. Let us denote the vertices that are adjacent to $v$ as $adj(v)$. For each $V_i$ in $C$, $V_i' = adj(v) \cap V_i$ is the set of adjacent vertices that are in the same independent set and they can share the same subset of subchannels. $\alpha(V_i')$ is the maximum weight of $v$'s adjacent vertices that *have not been* assigned subchannels yet. $\alpha(V_i')$ is the *contending load* of independent set $V_i$ to $v$. Therefore, the sum of contending load to $v$ is $\sum_{i=0}^{k}(\alpha(V_i'))$. The number of available subchannels that are assigned to $v$ is $avail = \lfloor \frac{\alpha(V_u)}{\sum_{i=0}^{k}(\alpha(V_i'))+w(v)} \cdot n \rfloor$, where $n$ is the total number of available subchannels. Since we assign subchannels in the descending order of $w(v)$, current $v$ must be the vertex with the maximum weight.

## VI. Evaluation

we evaluate the performance of our interference identification and resource assignment through extensive simulations.

### A. Interference Identification

The simulation steps are outlined as follows. First, we create an area and deploy a femtocell network $N = \{F, M\}$, where $F$ and $M$ are femtocells and MSs at random locations. Each femtocell is assigned with a random number of MS (between 1 to 4) and each MS is associated with exactly one femtocell. Second, according to their location and the path loss function, we compute the RSS between every femtocell-MS pair. We define an interfering threshold $\Gamma$, such that if the RSS of a femtocell $f$ ($f \neq f(m)$) to an MS $m$ is above $\Gamma$, $f$ is regarded as a $real$ interferer to $m$. The set of real interferers to $m$ is denoted as *interferer(m)*. Third, in each frame, the simulator generates a transmission pattern for each femtocell. Based on the RSS and the transmission patterns, the simulator computes the received patterns on each MS. Finally, from these transmission and received patterns, we invoke the identification procedure to identify the interference relations in the network.

Note that the threshold $\Gamma$ here is only used to "create real interferers". These real interferers are what we want to identify without knowing or utilizing $\Gamma$. We want to detect the real interferers using our interference identification method. In real world, we do not need to "create" interferers. Any femtocell that is constantly causing interference to MSs is what we want to identify. The pass loss function between a femtocell and an MS account for indoor propagation is defined as $46.4 + 20 \cdot log_{10}(R) + 20 \cdot log_{10}(\frac{f}{5})$ [18] where $R$ is the distance between femtocell and MS in meters and $f$ is the center frequency in GHz, which is 5.3 GHz in our experiments.

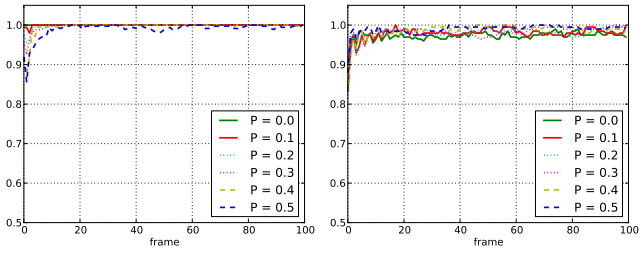


Fig. 7: Interference Identification for 100 frames. Left: $R_d$. Right: $R_e$. $|F| = 50$, $\theta = -87$ $dB$ and $|p| = 60$.

*1) Simulating the Patterns:* In our simulation, the received pattern is affected by real interferers. For example, if $p_{tx}(f(m)) = 00000111111111$, then $p_{rx}(m)$ should be 00000111111111. We set the interfering threshold to $\Gamma$ to $-85$ $dB$. For each real interferer $f$ in *interferer(m)*, it causes interference on $m$ and we update $p_{rx}(m)$ according to $p_{tx}(f)$. Suppose $m$ is experiencing interference from an interferer $f$ with $p_{tx}(f) = 11111111100000$. $p_{rx}(m)$ is updated to

000000000011111.

However, several factors affect wireless links. It is not sufficient to generate the received pattern merely by the aforementioned method. It is possible that a real interferer to $m$ is only affecting part of the subchannels of $m$ because this real interferer is a weak interferer to $m$. It is also possible that the RB carried by subchannel $m$ is dropped because the wireless link between $m$ and $f(m)$ becomes weak (such as due to frequency selective fading), not because of any interferer. We model such uncertainty by applying an *error probability P* that randomly flips 1s to 0s in $p_{rx}$. Note that an MS $m$ does not receive RBs that are not meant for it and thus flipping 0s to 1s in $p_{rx}$s should not be performed.

*2) Evaluation Metrics:* We define two metrics to evaluate the performance of our interference identification method.

$$detection\ rate: R_d = \frac{d}{\sum_{i=0}^{|M-1|} interferer(m_i)} \quad (1)$$

$$exclusion\ rate: R_e = \frac{e}{\sum_{i=0}^{|M-1|} irrelevant(m_i)} \quad (2)$$

where $d$ is the total number of real interferers successfully detected and $e$ is the number of non-interferers (denoted as *irrelevant*$(m_i)$ = *suspect*$(m_i)$ − *interferer*$(m_i)$) successfully identified by our method.

Both metrics are the higher the better, but $R_d$ is more important than $R_e$. If $R_d$ is not 100%, it means that there are some real interferers that are not detected correctly. Failing to detect all real interferers may result in interference between $f$ and $f(m)$. On the other hand, it is less severe if $R_e$ is not 100%. As mentioned in Section IV, the worst case performance is bounded by identifying all $f \in$ *suspect*$(m)$ as interferers to $m$. The worst case performance means $R_e = 0$, all of the non-interfering femtocells are misidentified as real interferers. It only falls back to identifying interferers based on the threshold of RSS.

*3) Evaluation:* We generate 10 random test cases in a $500 \cdot 500$ $m^2$ area for each femtocell density setting (10 to 50 femtocells in the area). The pattern length $|p|$ in WiMAX can be 15, 30 or 60. We simulate each of the test cases 10 times with different *error probability* $P$ and $|p|$ for 100 frames. The *error probability* $P$ varies from 0 to 0.5, increment by 0.05. The simulation results are shown in Figure 6. Each block denotes the average of all 10 runs of 10 test cases and the darker the block is, the lower the $R_e$ and $R_d$ is.

Considering the simulation of 50 femtocells, $(\theta, |p|, P) = (-87\ dB, 15, 0.0)$, $R_e$ is 63.2% and $R_d$ is 100%, which means that all real interferers are detected correctly and 63.2% of the non-interfering femtocells are identified as non-interferers. $R_d$ is always 100% if $P$ is below 0.2, which roughly means that if there are less than 20% of error bits in $p_{rx}$, we can identify *all* real interferers. It is inevitable that when $P$ increases, the number of bad bits increases and $R_d$ decreases. The pattern becomes meaningless as $P$ increases because the BDR difference is no longer mainly caused by designed interference. However, in our interference experiment in Section III, the error probability is at most 10%. The proposed interference identification works well in this condition.

One might notice that when there are more femtocells in the area, $R_e$ increases along with $P$ (vertical direction in each graph). However, it does not mean better identification performance. We should also take the corresponding $R_d$ into consideration for high femtocell density and high $P$. Considering both $R_d$ and $R_e$, we can see that the identification is now ineffective. With a higher error probability $P$, it starts to mistakenly identify real interferers as non-interferers.

On the other hand, $R_e$ decreases while the density of femtocell increases (horizontal direction in each graph) and the decrement of $R_d$ is less significant. It is because there is only limited number of bits in a pattern. Higher femtocell density means more potential interferer and the possibility of collision is higher. If $p_{rx}(m) = 0_n$, we cannot extract much useful information from $0_n$. Recall that when there are bad bits in a pattern and $p_{free}$ is not sufficient for our goal, we rely on $p_{ux}$, $p_{cx}$ and $p_{irr}$ to identify the interferer. As the density of femtocell increases, the chance that we have a useful $p_{ux}$ decreases and we cannot extract $p_{cx}$ and $p_{irr}$. It leaves us no choice but to assume that the suspicious interferer is a real interferer. For $|p| = 15$, $R_e$ drops as the femtocell density increases, which means more non-interfering femtocells are misidentified as interferers. However, note that our method still effectively identifies 56.9% of non-interferers in $(\theta, |p|, P) = (-89\ dB, 15, 0.0)$. The performance is expected to be improved if there are more subchannels ($|p|$ gets longer). With more subchannels, the chance that a received pattern becomes $0_n$ becomes lower and more useful information can be extracted and it is confirmed in Figure 6.

Figure 7 shows a simulation of 50 femtocells for 100 frames. The interference identification quickly becomes stable within 20 frames. Although we set the length of the record to 40, our method only need less than 20 frames to achieve a stable

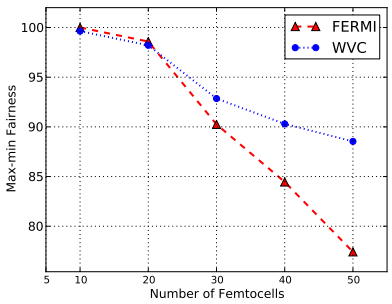


Fig. 8: Max-min fairness

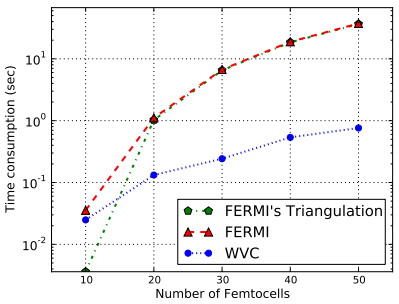


Fig. 9: Time consumption

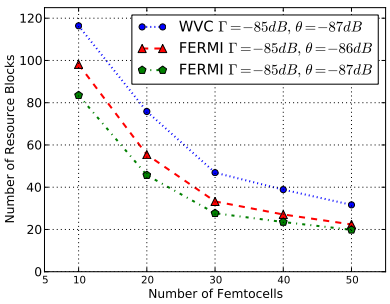


Fig. 10: Throughput comparison

identification. The frame length of OFDMA systems vary from 2 to 20 ms, which means our method is able to achieve stable identification in less than 400 ms. Therefore, our method is able to handle the network dynamics in cellular networks.

### B. Resource Allocation and Assignment

The central controller constructs the conflict graph as it identifies the interferers. The fairness and the time consumption for the test cases where $\Gamma = -85\ dB$, $\theta = -87\ dB$ and $|p| = 60$ are shown in Figure 8 and 9. In both figures, the blue and red curves represent WVC algorithm and FERMI, respectively. Each point on the curves is the average of all 10 test cases with certain femtocell density. For low femtocell density, the generated conflict graphs are usually simple chordal graphs and FERMI can achieve optimal fairness assignment easily. However, the possibility that the input graph is non-chordal increases drastically along with the size of the graph. It requires triangulation [16] to add the fill-in edges to make the input graph chordal and brings two side effects. (1) First, the extra fill-in edges degrades the fairness significantly as the size of the graph grows. (2) Second, the triangulation algorithm [16] involves paths with special property and can be very time consuming in large graphs. As we can see in Figure 9, the green curve represents the time consumption of the triangulation algorithm. The time consumption of FERMI is dominated by the triangulation algorithm. Our WVC algorithm in low femtocell density has slightly lower fairness, but in overall our WVC algorithm outperforms maximal clique method in terms of efficiency.

The throughput comparisons are shown in Figure 10. There are 30 subchannels and 12 RBs per subchannel in a frame. The blue curve represents the throughput of WVC algorithm. The red and green curve represent the throughput of FERMI's algorithm under different parameters. Each point denotes the average of 10 test cases with certain femtocell density. Higher femtocell density results in less RB acquired by the MS. In simulations with $|p|$ equal to 30, more than $75\%$ non-interferers are identified and the number of edges in our conflict graph decreases significantly. In contract, FERMI can only conservatively set the femtocells with RSS higher than the suspect threshold $\theta$ as interferers and the performance is reduced due to those unnecessary edges in the conflict graph. Even $\theta$ is set to *-86 dB* the throughput is still lower than the proposed WVC algorithm with our interference identification.

## VII. Conclusion

Identifying interference in femtocell network is the most critical step that directly affects the performance of resource allocation. In this paper, we propose an efficient method that takes advantage of the availability of multiple subchannels to identify the inter-femtocell interference by generating received patterns on the MSs. These patterns are then collected at a central controller where interference relations are identified. We conduct experiments on USRP to show the generations of received patterns on MSs. We simulate our interference identification method and demonstrate that if the error probability is less than 0.2, our method successfully identifies *all* real interferers and *at least 60%* of the non-interferers. Moreover, the method achieves a stable identification in less than 20 frames. We also propose a weighted vertex-coloring (WVC) based resource assignment algorithm that achieves better fairness for higher density networks in less time compared with FERMI. In addition, without adding unnecessary edges in the conflict graph, the throughput is also improved.

## References


[1] V. Chandrasekhar, J. Andrews, and A. Gatherer, "Femtocell networks: a survey," *Communications Magazine, IEEE*, vol. 46, no. 9, pp. 59–67, september 2008.

[2] R. v. Nee and R. Prasad, *OFDM for Wireless Multimedia Communications*, 1st ed. Norwood, MA, USA: Artech House, Inc., 2000.

[3] H. Claussen, "Performance of macro- and co-channel femtocells in a hierarchical cell structure," in *Personal, Indoor and Mobile Radio Communications, 2007. PIMRC 2007. IEEE 18th International Symposium on*, sept. 2007, pp. 1–5.

[4] V. Chandrasekhar and J. G. Andrews, "Uplink capacity and interference avoidance for two-tier femtocell networks," *Trans. Wireless. Comm.*, vol. 8, no. 7, pp. 3498–3509, Jul. 2009.

[5] J.-S. Wu, J.-K. Chung, and M.-T. Sze, "Analysis of uplink and downlink capacities for two-tier cellular system," *Communications, IEE Proceedings-*, vol. 144, no. 6, pp. 405–411, dec 1997.

[6] K. Sundaresan and S. Rangarajan, "Efficient resource management in ofdma femto cells," in *Proceedings of the tenth ACM international symposium on Mobile ad hoc networking and computing*, ser. MobiHoc '09. New York, NY, USA: ACM, 2009, pp. 33–42.

[7] M. Y. Arslan, J. Yoon, K. Sundaresan, S. V. Krishnamurthy, and S. Banerjee, "Fermi: a femtocell resource management system forinterference mitigation in ofdma networks," in *Proceedings of the 17th annual international conference on Mobile computing and networking*, ser. MobiCom '11. New York, NY, USA: ACM, 2011, pp. 25–36.

[8] H. Rahul, N. Kushman, D. Katabi, C. Sodini, and F. Edalat, "Learning to share: narrowband-friendly wideband networks," *SIGCOMM Comput. Commun. Rev.*, vol. 38, no. 4, pp. 147–158, Aug. 2008.

[9] R. Chang, Z. Tao, J. Zhang, and C.-C. Kuo, "A graph approach to dynamic fractional frequency reuse (ffr) in multi-cell ofdma networks," in *Communications, 2009. ICC '09. IEEE International Conference on*, june 2009, pp. 1–6.

[10] T. Quek, Z. Lei, and S. Sun, "Adaptive interference coordination in multi-cell ofdma systems," in *Personal, Indoor and Mobile Radio Communications, 2009 IEEE 20th International Symposium on*, sept. 2009, pp. 2380–2384.

[11] A. Galindo-Serrano and L. Giupponi, "Distributed q-learning for interference control in ofdma-based femtocell networks," in *Vehicular Technology Conference (VTC 2010-Spring), 2010 IEEE 71st*, May 2010, pp. 1–5.

[12] J. Yoon, M. Y. Arslan, K. Sundaresan, S. V. Krishnamurthy, and S. Banerjee, "A distributed resource management framework for interference mitigation in ofdma femtocell networks," in *Proceedings of the thirteenth ACM international symposium on Mobile Ad Hoc Networking and Computing*, ser. MobiHoc '12. New York, NY, USA: ACM, 2012, pp. 233–242.

[13] E. Blossom, "Gnu radio: tools for exploring the radio frequency spectrum," *Linux J.*, vol. 2004, no. 122, p. 4, Jun. 2004.

[14] "Universal software radio peripheral," http://www.ettus.com/.

[15] R. Jain, A. Durresi, and G. Babic, "Throughput fairness index: An explanation," in *TM Forum Document Number: ATM Forum / 990045*, Feb 1999.

[16] A. Berry, J. R. S. Blair, P. Heggernes, and B. W. Peyton, "Maximum cardinality search for computing minimal triangulations of graphs," in *ALGORITHMICA*. Springer Verlag, 2002, pp. 1–12.

[17] A. Mishra, S. Banerjee, and W. Arbaugh, "Weighted coloring based channel assignment for wlans," *SIGMOBILE Mob. Comput. Commun. Rev.*, vol. 9, no. 3, pp. 19–31, Jul. 2005.

[18] S. ping Yeh, S. Talwar, N. Himayat, and K. Johnsson, "Text proposal on hierarchical networks simulation methodology," September 2010.